

# Intratumoral injection of radioactive Astatine ( $^{211}\text{At}$ ) microspheres for the treatment of tumors

Y. Li<sup>1</sup>, F. Pang<sup>2</sup>, H. Cai<sup>1</sup>, L. Li<sup>\*</sup>

<sup>1</sup>Department of Nuclear Medicine, West China Hospital of Sichuan University, China

<sup>2</sup>Department of Intervention, Shenzhen Traditional Chinese Medicine Hospital, China

## ► Original article

### \*Corresponding author:

Lin Li, M.D.,

E-mail: tsflyh@126.com

Received: August 2021

Final revised: April 2022

Accepted: May 2022

Int. J. Radiat. Res., October 2022;  
20(4): 793-798

DOI: 10.52547/ijrr.20.4.10

**Keywords:** Brachytherapy, microspheres, radiation oncology, Astatine-211.

## ABSTRACT

**Background:** Our aims were to prepare microspheres labelled with radioactive astatine as brachytherapy seeds and to confirm the antitumor ability of these microspheres. **Materials and Methods:** Chitosan-collagen composite microspheres (CCMs) were synthesized through an emulsification crosslink reaction and radiolabelled with  $^{211}\text{At}$  using the chloramine-T method. Radiation stability was assessed in both phosphate-buffered saline and blood serum. The in vivo distribution and therapeutic effects were evaluated in BALB/c nude mice with implanted tumours. **Results:** CCMs showed ideal morphological characteristics (diameter of 7.5-15  $\mu\text{m}$ ) and acceptable radiation stability (73.99% in PBS and 72.56% in serum after 16 hours). The in vivo biodistribution analysis demonstrated that  $^{211}\text{At}$ -CCMs were highly localized in tumour tissue. The therapeutic efficacy of  $^{211}\text{At}$ -CCMs when intratumorally injected into a cervical tumour model was assessed. Fourteen days after a single-dose treatment with  $^{211}\text{At}$ -CCMs, significantly retarded tumour volume growth was observed. **Conclusion:**  $^{211}\text{At}$ -CCM brachytherapy has the potential to provide an alternative solution for tumour treatment.

## INTRODUCTION

Together with surgery and chemotherapy, radiation therapy is effective in the clinical treatment of cancer, especially in radiation-sensitive tumours (1). High-dose ionizing radiation therapy induces cell death and limits the proliferation and regeneration of tumours. Internal radiation therapy, which is also referred to as brachytherapy, involves using minimally invasive procedures to place a radiation source inside or nearby the tumour. Therefore, a continuous radiation dose is commonly applied either by temporary implants (short-term therapy) or permanent implants (lifetime therapy until complete decay of the tumour) (2). Brachytherapy, which is safe for normal tissues, can effectively confine the therapeutic radiation dose to the limited region of the tumour. It has the advantages of fewer side effects, shorter treatment duration and cost-effectiveness due to its ability to accurately target tumours (3). Thus, brachytherapy has become an optional standard therapy for many malignant tumours.

Three categories of brachytherapy seeds exist: millimetres, micrometers and nanosizes. Millimetre seeds for brachytherapy are commonly used in prostate cancer treatment via surgical implantation, which causes various side effects and severely limits their clinical application (4-6). A majority of patients experience side effects and severe complications after surgical implantation because of the size of the

millimetre seeds (7, 8). Micrometer- and nanoscale seeds can be injected through much smaller needles, which reduces the lesions caused by surgical implantation. Meanwhile, it is easy to set different radiation dosages by applying different numbers of seeds. Nanoscale brachytherapy seeds have undergone rapid development in recent years. Due to the extraordinary treatment outcomes, radioactive nanoparticles can be used as a potential alternative to conventional brachytherapy (9). As reported by Laprise-Pelletier, a new brachytherapy was developed based on intratumoral injection of radioactive Au nanoparticles for prostate cancer treatment. Salvanou verified the effectiveness of Au nanoparticles radiolabelled with the alpha-emitter actinium-225 (10, 11). However, there is a risk of nanoparticles diffusing away from the target because of the extremely small size of nanoseeds. Micrometer radiation particles are currently used in intraarterial transcatheter radioembolization treatment of liver cancer (12). Recently, S. A. van Nimwegen confirmed that  $^{166}\text{Ho}$  microbrachytherapy has potential as a minimally invasive, single-procedure radioablation treatment for tumours with minimal morbidity (13). With the advantages of being injectable by needles and less diffusion away from the target tissue, microbrachytherapy has attracted increasing attention for the treatment of solid tumours.

Compared with  $\beta$ - and  $\gamma$ -emitters,  $\alpha$ -particles emit radiation with high linear energy transfer. In addition,  $\alpha$ -particles have high relative biological

efficiency is because their cytotoxic efficiency is not dependent on the dose rate, oxygen concentration or cell cycle status <sup>(14)</sup>. Astatine-211, <sup>213</sup>Bi, <sup>212</sup>Bi, <sup>223</sup>Ra, and <sup>225</sup>Ac are the most commonly studied  $\alpha$ -particle emitting radionuclides for radiotherapy <sup>(15)</sup>. Due to its relatively long half-life, 100% of its decay to  $\alpha$ -emission and good imaging feasibility, astatine-211 is potentially the most promising agent for  $\alpha$ -particle therapies. Recently, astatine-211 has been used to label different molecules, such as inhibitors of prostate-specific antigens, amino acid transporter substrates, and antibodies targeting specific tumour surface ligands for alpha therapy of tumours through intravenous injection or gold nanoparticles for alpha therapy via intratumoral administration <sup>(16, 17)</sup>.

In our previous research, we reported (131) iodine-labelled chitosan-collagen composite microspheres (CCMs) and verified their potential for radioembolization interventional hepatocellular carcinoma therapy <sup>(18)</sup>. As biodegradable organic polymer materials with many advantages, chitosan and collagen have been widely used in biomedical fields. However, (131) iodine emits both  $\beta$  and  $\gamma$  rays and could lead to unnecessary radiation exposure. On the other hand, as far as we know, no treatments for antineoplastic tumours using astatine-211-labelled biodegradable microspheres for alpha therapy via intratumoral administration have been reported thus far. Therefore, in this study, we attempted to use the radionuclide astatine-211 to label CCMs and verified the microbrachytherapy ability of these CCMs in solid tumours. Overall, the purpose of this study was to prepare biodegradable microspheres labelled with <sup>211</sup>At and confirm their antitumor ability.

## MATERIALS AND METHODS

### Major chemicals, reagents and equipment

Type I collagen was obtained from Corning (Corning, NY, USA). Chitosan (median molecular weight, 190-310 kDa, 75%-85% deacetylated), phosphate-buffered saline (PBS), liquid paraffin, sorbitan monooleate (Span-80), isopropyl alcohol, glutaraldehyde (50%, C<sub>2</sub>H<sub>8</sub>O<sub>2</sub>), chloramine T trihydrate and sodium pyrosulfite (Na<sub>2</sub>S<sub>2</sub>O<sub>5</sub>) were purchased from Sigma-Aldrich (Saint Louis, MO, USA). Centrifuge tubes and micropipettors were purchased from Corning (Corning, NY, USA). <sup>211</sup>At was supplied by the Institute of Nuclear Science and Technology, Sichuan University. All aqueous solutions were prepared in threefold-distilled water that was obtained from a Direct-Q8 UV-R water system (Merck KGaA, Germany). Dulbecco's modified Eagle's medium (DMEM high glucose), foetal bovine serum, trypsin-EDTA solution and penicillin-streptomycin solution were obtained from GE Healthcare (GE, USA).

Information concerning the other major equipment used is listed as follows: scanning electron

microscopy (SEM; JSM-390LV, JEOL, Tokyo, Japan); radioactive thin-layer chromatography (TLC; FC3600, Bioscan, USA); radioactivity metre (RM905a, Beijing Hicheer Sci-Tec Co., Ltd, CN); orthotopic light microscope (DM500, Leica, Germany); electronic balance (ESJ120-4, Longteng Electronics Co., Ltd, CN); high-pressure steam sterilizer (MLS-3781L, PHC Group, Japan); table-top high speed centrifuge (Minimax21, BioMaker, CN); electron microscope (JSM-390LV, JEOL, Japan); freeze drier (FD-1A-50, BIOCOOL, Beijing, CN); laser particle size analyser (JL-6000, JNGX, Chengdu, CN); carbon dioxide cell incubator (MCO-18AC, Panasonic, Japan).

### Preparation and characterization of CCMs

Briefly, CCMs were synthesized through an emulsification crosslink reaction. First, 8 mg of chitosan was dissolved in 4 mL of type I collagen water solution (4 mg/mL) and added dropwise into 18 mL of liquid paraffin containing 720  $\mu$ L of Span-80 under stirring at 1000 rpm for 1 h at room temperature to form the w/o emulsion. Second, 500  $\mu$ L of glutaraldehyde was added dropwise into the emulsion and stirred continuously for 1 h to catalyse crosslinking and solidification of microspheres. Next, the CCMs were washed several times with isopropanol to completely remove the oil phase. Then, the CCMs were sterilized in an autoclave (121 °C, 15 min) and freeze-dried for further use. The morphological characteristics of the CCMs were investigated via SEM. The average size of the CCMs was determined using a laser particle size detector.

### Radiolabelling of <sup>211</sup>At-CCMs

Briefly, 10 mg of CCMs was dissolved in 500  $\mu$ L of threefold-distilled water with 7.4 MBq of <sup>211</sup>At (0.074 MBq/ $\mu$ L) and 20  $\mu$ L of chloramine-T solution (20 mg/mL). The mixture was stirred for 5 min and incubated for 25 min at room temperature for the reaction. Subsequently, 10  $\mu$ L of sodium pyrosulfite solution (15 mg/mL) was added to stop the reaction. The product was washed with saline over five times and then stored for further testing. Radioactive TLC and a radioactivity metre were used to evaluate the radiochemical yield. Then, the <sup>211</sup>At-CCMs (3.7 MBq, centrifuged and washed, nearly 100% radiochemical purity at initial time) were incubated with an equal volume of PBS or rat blood serum at 37 °C, and the radiochemical purities were monitored by TLC for up to 16 h.

### Animals and tumour modelling

All animals were kept in laminar flow cages at a temperature of 22  $\pm$  2 °C and humidity of 50-60% under an ambient photoperiod. Every four mice were maintained in one cage for one week to acclimatize. A thermostatic blanket for mouse placement and 2% isoflurane for anaesthesia were utilized during all invasive manipulations. A total of twenty-six mice were used for experiments. Six mice were used for

biodistribution, and twenty mice were used for therapeutic evaluation.

HeLa and human cervical cancer cells were obtained from the American Type Culture Collection (ATCC) and cultured in DMEM high glucose supplemented with 10% (v/v) foetal bovine serum (FBS) and 1% penicillin-streptomycin solution in an incubator (37 °C, 5%  $\text{CO}_2$ ). Culture medium was replaced every 48 h, and the cells were collected in the exponential growth phase using trypsin-EDTA solution, washed twice with precooled PBS, and suspended in PBS ( $5 \times 10^7$  cells/mL) for further experiments.

Tumours were induced as follows: a cell suspension containing  $5 \times 10^6$  HeLa cells (approximately 100  $\mu\text{L}$  in volume) was implanted subcutaneously into the left shoulder of BALB/c nude mice. Tumour growth lasted for 2 weeks to reach a palpable size (approximately 5-6 mm in diameter).

#### Biodistribution assessment of $^{211}\text{At}$ -CCMs

The biodistribution of  $^{211}\text{At}$ -CCMs was assessed to examine the stability of  $^{211}\text{At}$ -CCMs in vivo. Approximately 25  $\mu\text{L}$  (370 KBq) of  $^{211}\text{At}$ -CCMs in physiological saline solution was injected intratumorally. At 0.5 h and 6 h following injection, the lungs, heart, blood, brain, spleen, liver, kidneys, stomach, intestine and muscle were removed, weighed and measured with a gamma counter ( $n=3$ ). All data were decay corrected to the time of administration.

#### Therapeutic evaluation

The following formula was used for tumour size (V,  $\text{mm}^3$ ) calculation:

$$V = (L \times W^2) / 2$$

W (width, cm) was the shorter and L (length, cm) was the longer of the two perpendicular tumour axes. Average tumour size (V,  $\text{mm}^3$ ) growth curves were calculated for each treatment group. Tumour growth was monitored for two weeks, and the mice were sacrificed humanely via an overdose of isoflurane. Then, tumours were collected, fixed in paraformaldehyde (24 h) and embedded in paraffin. Consecutive slices (5  $\mu\text{m}$ ) were processed for haematoxylin and eosin (H&E) staining for pathological examination using an orthotopic light microscope.

#### Statistical analysis

Statistical processing was performed using SPSS 22.0. To evaluate the tumour volume, statistical analysis included calculation of average and standard deviation (SD).

## RESULTS

#### Characterizations of CCMs

CCMs were successfully prepared using the emulsification and chemical crosslinking method. The scanning electron microscopy (SEM) results for the

CCMs are shown in figure 1. The majority of CCMs had diameters of 7.5-15  $\mu\text{m}$ .

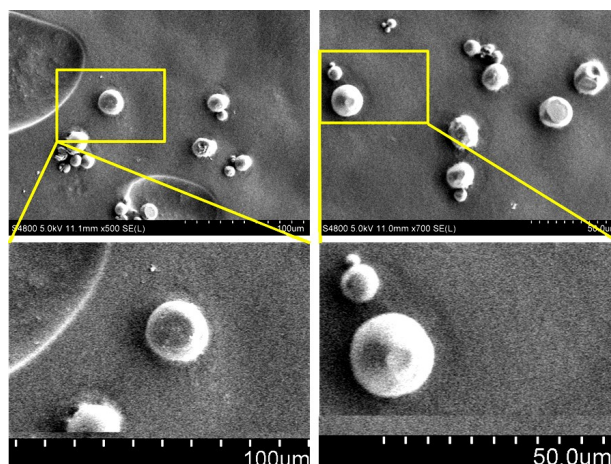


**Figure 1.** SEM images of CCMs. The scale bar was shown on the below of each figure.

#### Radiolabelling in-vitro

A radiolabelling yield of 84.43% was determined using radioactive TLC and a radioactivity metre (figure 2A). Then, as shown in figure 2B, favourable stability of  $^{211}\text{At}$ -CCMs was observed in both PBS and blood serum. The radiochemical purities of  $^{211}\text{At}$ -CCMs dropped to 73.99% in PBS and 72.56% in blood serum after 16 h, which is a period of over 2 half-lives of  $^{211}\text{At}$ .

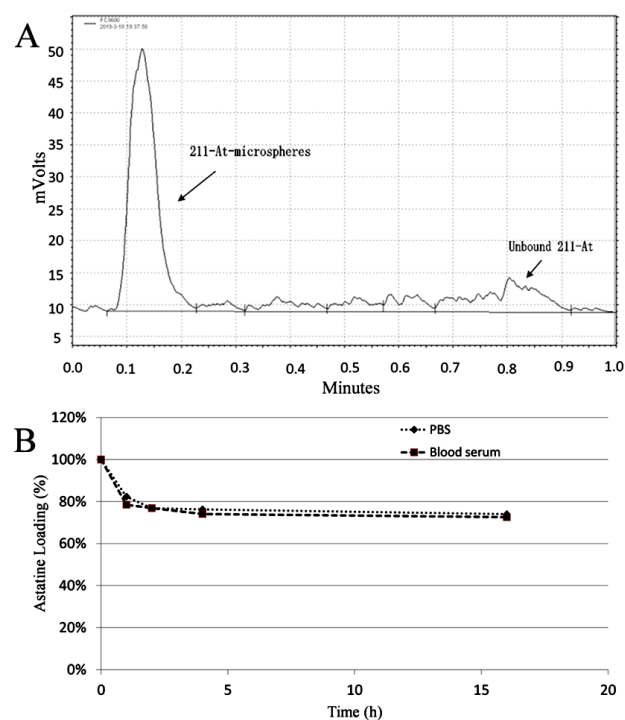


**Figure 2.** TLC results (A) and radiation stability (B).

#### Biodistribution

The biodistribution of  $^{211}\text{At}$ -CCMs was determined at 0.5 h and 6 h post-injection. The biodistribution results are presented in figure 3. Data are presented as the average  $\pm$ SD ( $n=3$ ). A high  $^{211}\text{At}$  activity concentration was found in tumour tissue at 0.5 h after injection. Extremely low activity concentrations



were observed in the lungs, heart, blood, brain, spleen, liver, kidneys, stomach, intestine and muscle tissues. Six hours after injection, the  $^{211}\text{At}$  activity concentration remained high in tumour tissue. A slightly increased activity concentration appeared in the other investigated tissues, especially blood, lung and bone.

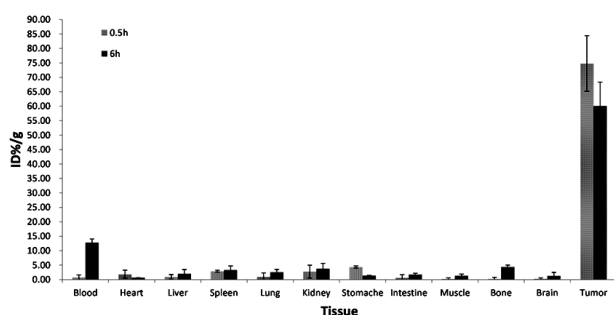


Figure 3. In-vivo distribution of  $^{211}\text{At}$ -CCMs.

### Antitumor effect of $^{211}\text{At}$ -CCMs

The curves of tumour volumes in the four groups of tumour-bearing mice are shown in figure 4. Data are presented as the average  $\pm$ SD ( $n=5$ ). At 14 days after intratumor injection, a clear separation in the tumour growth profile was observed. As expected, the group treated with  $^{211}\text{At}$ -CCMs in PBS suspension exhibited significantly retarded tumour volume growth, while the tumours showed rapid growth in both the PBS solution- and CCMs in PBS suspension-treated groups. The group treated with  $^{211}\text{At}$  in PBS solution showed intermediate tumour volume growth.

The results of pathological analysis of tumour tissues after intratumoral injection in the four groups are displayed in figure 5. Blue arrows indicate microspheres. Karyopyknosis and necrotic processes in tumour tissue could be observed around the  $^{211}\text{At}$ -CCMs (figure 5A). The tumour tissue near CCMs showed mild fibrosis (figure 5B). In the group treated with  $^{211}\text{At}$  in PBS, a portion of tumour tissue showed necrotic changes (figure 5C). The pathology results confirmed that  $^{211}\text{At}$ -CCMs had the most efficient antitumor ability.

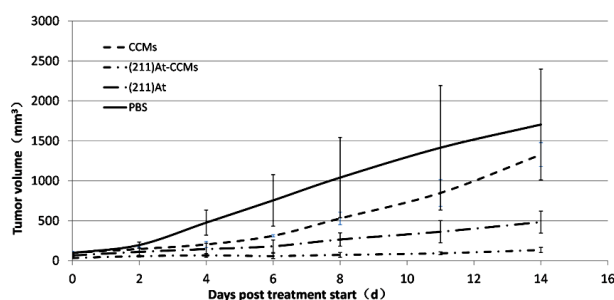


Figure 4. Tumour volume changes after intratumor injection.

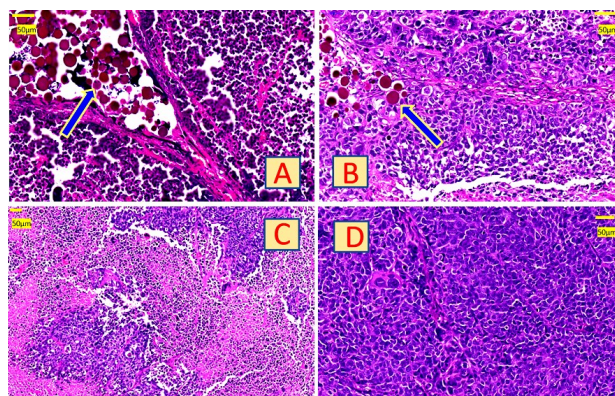


Figure 5. Pathology assessment of therapeutic efficacy. Blue arrows indicate the microspheres. (A)  $^{211}\text{At}$ -CCM administration, (B) CCM administration, (C)  $^{211}\text{At}$  administration, and (D) PBS administration. The scale bar was shown on the front of each figure.

## DISCUSSION

In brachytherapy, radioactive sources are placed accurately and directly inside or by the tumour. The method is suitable for patients with different types of cancer. Therefore, this method is commonly requested by patients either as an essential or as a part of their clinical treatment. According to a review by Chargari, brachytherapy, with high-level evidence from randomized controlled trials, is recommended in 1) patients with locally advanced cervical cancer together with chemoradiation; 2) postoperative patients with uterine endometrial cancer to reduce the risk of vaginal vault recurrence; 3) patients with high-risk prostate cancer to perform dose escalation and improve progression-free survival; and 4) patients with breast cancer as an adjuvant to accelerate partial breast irradiation or to boost the tumour bed <sup>(19)</sup>. Therefore, brachytherapy has a good chance of success in both primary tumours and residual tumour margins after debulking surgery.

The dose of radioactivity in brachytherapy is an essential factor. Yasuhiro Ohshima designed a study to assess the therapeutic effects of  $^{211}\text{At}$ -astato-benzylguanidine ( $^{211}\text{At}$ -MABG) <sup>(20)</sup>. Pheochromocytoma tumour-bearing mice received intravenous injections of  $^{211}\text{At}$ -MABG (0.28, 0.56, 1.11, 1.85, 3.70 and 5.55 MBq; five mice per group). The group treated with 0.28, 0.56 and 1.11 MBq of  $^{211}\text{At}$ -MABG showed significantly lower relative tumour growth during the first 38 days than the control group, with only a temporary weight loss, which was restored by Day 10. Yasuhiro Ohshima concluded that the maximal tolerated dose of  $^{211}\text{At}$ -MABG in nude mice was 1.11 MBq. R H Larsen reported a study of  $^{211}\text{At}$ -particles in a murine intraperitoneal tumour model <sup>(21)</sup>, and radioactivity values of 0.5 and 0.2 MBq of  $^{211}\text{At}$ -particles were adopted for treatment. Referring to previous studies,

each tumour-bearing mouse received 0.555 MBq <sup>211</sup>At-particles in our study. And the results confirmed 0.555 MBq of <sup>211</sup>At particles was suitable and effective for tumour treatment.

Collagen and chitosan are considered promising candidates for brachytherapy microspheres due to their ideal biocompatibility, nontoxicity, and biodegradability (22, 23). As a natural polymer (2-amino-2-deoxy-d-glucopyranose), chitosan can be used as a raw material for microspheres for drug delivery. The abundant amino acid residues of collagen allow the labelling of radioisotopes. In our study, a <sup>211</sup>At radiolabelling yield of 84.43% was achieved in chitosan-collagen microspheres, and a slight drop in radiochemical purity was observed in both PBS and blood serum. The biodistribution results also verified that a small portion of <sup>211</sup>At-CCMs were not stable after intratumoral injection, although the majority of radioactivity remained in tumour tissue. Almut Walte reported <sup>211</sup>At-labelled antineoplastic antibodies, and the stability of these <sup>211</sup>At antibodies in murine serum exceeded 85% at 37 degrees after 21 hours (24). Monika Lyczko attempted to label substance P (SP) with <sup>211</sup>At in their research, and the stability of the compound in PBS was high (37 degrees, 20 hours, 91.3 ± 1.3%) (25). By comparison, in our research, the stability of <sup>211</sup>At-CCMs (16 hours, 73.99% in PBS and 72.56% in blood serum) required improvement in subsequent studies.

Only a few antitumour studies on <sup>211</sup>At-particles have been reported. Most recently, Hiroki Kato reported astatine-211-labelled gold nanoparticles and concluded that the intratumoral single administration of these simple nanoparticles strongly suppressed the growth of tumour tissue without radiation exposure to other organs as a consequence of the systemic spread of radionuclide (17). This result is in accordance with our study. Several studies on α-ray-emitting particles in addition to astatine-211 have also been reported. Salvanou indicated that α-ray-emitting nuclide <sup>225</sup>Ac-labelled AuNPs are potentially useful to inhibit tumour growth after intratumoral administration in glioma xenografts (26). A study reported by Muslimov verified the efficacy of intratumoral administration of <sup>225</sup>Ac-doped core-shell submicron CaCO<sub>3</sub> particles for local α-radionuclide therapy (27). These studies indicated that α-ray-emitting particles produce satisfactory retention ability, safety and effectiveness in inhibiting tumour growth.

## CONCLUSION

We developed a novel composite biomaterial, collagen-chitosan microspheres (CCMs). The CCMs demonstrate good <sup>211</sup>At labelling efficiency and ideal stability both in vivo and in vitro. The <sup>211</sup>At-CCMs showed effective antitumor ability and potential for

application in brachytherapy for tumours. Further studies should be performed to improve the stability of <sup>211</sup>At-CCMs and expand their clinical application.

## ACKNOWLEDGEMENTS

The authors wish to thank Doc. Liu Xiao and Mufeng Li for their skillful handling of the animals, sample collection and tissue processing. We would like to thank Yu Tang and Weihao Liu at the Institute of Nuclear Science and Technology of Sichuan University for providing <sup>211</sup>At.

**Conflicts of interest:** Declared none.

**Ethical approve:** All animal care and experimental procedures were approved by the Clinical Trials and Biomedical Ethics Committee, West China Hospital of Sichuan University on 23rd February 2021. The approved number of ethic committee is 2021207A.

**Funding:** No funding was received in this study.

**Author contribution:** Y.L. and F.P prepared the CCMs together. Y.L. performed all in vivo and vitro experiments (histology, tumor efficiency evaluation, SEM, radiolabeling). F.P. assisted with in vitro experiments and H.C. assisted with in vivo experiments. Y.L. and L.L. prepared and wrote the final version of the manuscript.

## REFERENCES

1. Wang JTW, Klippstein R, Martincic M, Pach E, Feldman R, Sefl M, Michel Y, Asker D, et al. (2020) Neutron activated Sm-153 sealed in carbon nanocapsules for in vivo imaging and tumor radiotherapy. *Acs Nano*, **14**(1): 129-141.
2. Moendarbari S, Tekade R, Mulgaonkar A, Christensen P, Ramezani S, Hassan G, Jiang R, Oez OK, Hao Y, Sun X (2016) Theranostic nanoseeds for efficacious internal radiation therapy of unresectable solid tumors. *Sci Rep*, **6**: 20614.
3. Otter SJ, Stewart AJ, Devlin PM (2019) Modern brachytherapy. *Hematol Oncol Clin N*, **33**(6): 1011.
4. Hannoun-Levi JM (2017) Brachytherapy for prostate cancer: Present and future. *Cancer Radiother*, **21**(6-7): 469-472.
5. Zaorsky NG, Davis BJ, Nguyen PL, Showalter TN, Hoskin PJ, Yoshiooka Y, Morton GC, Horwitz EM (2017) The evolution of brachytherapy for prostate cancer. *Nat Rev Urol*, **14**(7): 415-439.
6. Bensaleh S, Bezak E, Borg M (2009) Review of MammoSite brachytherapy: Advantages, disadvantages and clinical outcomes. *Acta Oncol*, **48**(4): 487-494.
7. McLaughlin PW and Narayana V (2020) Progress in Low Dose Rate Brachytherapy for Prostate Cancer. *Semin Radiat Oncol*, **30**(1): 39-48.
8. Peschel RE, Colberg JW, Chen Z, Nath R, Wilson LD (2004) Iodine 125 versus palladium 103 implants for prostate cancer: Clinical outcomes and complications. *Cancer J*, **10**(3): 170-174.
9. Wu S, Helal-Neto E, Matos, APDS Jafari A, Kozempel J, Silva YJDA, Serrano-Larrea C, et al. (2020) Radioactive polymeric nanoparticles for biomedical application. *Drug Deliv*, **27**(1): 1544-1561.
10. Laprise-Pelletier M, Simao T, Fortin M (2020) Gold nanoparticles in radiotherapy and recent progress in nanobrachytherapy. *Adv Healthc Mater*, **7**(16): e1701460.
11. Salvanou E, Stellas D, Tsoukalas C, Mavroidi B, Paravatou-Petsotas M, Kalogeropoulos N, et al. (2020) A proof-of-concept study on the therapeutic potential of Au nanoparticles radiolabeled with the alpha-emitter Actinium-225. *Pharmaceutics*, **12**(2): 188.
12. Lee EJ, Chung HW, Jo JH, So Y (2019) Radioembolization for the treatment of primary and metastatic liver cancers. *Nucl Med Mol Imaging*, **53**(6): 367-373.
13. van Nimwegen SA, Bakker RC, Kirpensteijn J, van Es RJJ, Koole R, Lam MGEH, et al. (2018) Intratumoral injection of radioactive holmium (Ho-166) microspheres for treatment of oral squamous

- cell carcinoma in cats. *Vet Comp Oncol*, **16**(1): 114-124.
14. Vaidyanathan G and Zalutsky MR (2008) Astatine radiopharmaceuticals: Prospects and problems. *Curr Radiopharm*, **1**(3): 177-177.
  15. Song H, Hobbs RF, Vajravelu R, Huso DL, Esaias C, Apostolidis C, Morgenstern A, Sgouros G (2009) Radioimmunotherapy of breast cancer metastases with alpha-particle emitter <sup>225</sup>Ac: comparing efficacy with <sup>213</sup>Bi and <sup>90</sup>Y. *Cancer Res*, **69**(23): 8941-8948.
  16. Ha H, Kwon H, Lim T, Jang J, Park SK (2021) Inhibitors of prostate-specific membrane antigen in the diagnosis and therapy of metastatic prostate cancer - a review of patent literature. *Expert Opin Ther Pat*, **31**(6): 525-547.
  17. Kato H, Huang X, Kadonaga Y, Katayama D, Ooe K, Shimoyama A, Kabayama K, et al. (2021) Intratumoral administration of astatine-211-labeled gold nanoparticle for alpha therapy. *J Nanobiotechnology*, **19**(1): 223.
  18. Pang F, Li Y, Zhang W, Xia C, He Q, Li Z, Xiao L, Song S, Dong P, Zhou H, Shao T, Cai H, Li L (2020) Biodegradable (131) Iodine-labeled microspheres: potential transarterial radioembolization biomaterial for primary hepatocellular carcinoma treatment. *Adv Healthc Mater*, **9**(13): e2000028.
  19. Chargari C, Deutsch E, Blanchard P, Gouy S, Martelli H, Guerin F, Dumas I, Bossi A, Morice P, Viswanathan AN, Haie-Meder C (2019) Brachytherapy: An overview for clinicians. *CA Cancer J Clin*, **69**(5): 386-401.
  20. Ohshima Y, Sudo H, Watanabe S, Nagatsu K, Tsuji AB, Sakashita T, Ito YM, Yoshinaga K, Higashi T, Ishioka NS (2018) Antitumor effects of radionuclide treatment using alpha-emitting meta-(211)At-astato-benzylguanidine in a PC12 pheochromocytoma model. *Eur J Nucl Med Mol Imaging*, **45**(6): 999-1010.
  21. Larsen RH, Hoff P, Vergote IB, Bruland OS, Aas M, De Vos L, Nustad K (1995) Alpha-particle radiotherapy with <sup>211</sup>At-labeled monodisperse polymer particles, <sup>211</sup>At-labeled IgG proteins, and free <sup>211</sup>At in a murine intraperitoneal tumor model. *Gynecol Oncol*, **57**(1): 9-15.
  22. Meyer M (2019) Processing of collagen-based biomaterials and the resulting materials properties. *Biomed Eng Online*, **18**(1): 24.
  23. Muxika A, Etxabide A, Uranga J, Guerrero P, de la Caba K (2017) Chitosan as a bioactive polymer: Processing, properties and applications. *Int J Biol Macromol*, **105**(Pt 2): 1358-1368.
  24. Walte A, Sriyapureddy SS, Korkmaz Z, Krull D, Bolte O, Hofmann M, Meyer GJ, Knapp WH (2007) Preparation and evaluation of <sup>211</sup>At labelled antineoplastic antibodies. *J Pharm Sci*, **10**(2): 277s-285s.
  25. Lyczko M, Pruszyński M, Majkowska-Pilip A, Lyczko K, Was B, Meczynska-Wielgosz S, et al. (2017) (211)At labeled substance P (5-11) as potential radiopharmaceutical for glioma treatment. *Nucl Med Biol*, **53**: 1-8.
  26. Salvanou EA, Stellas D, Tsoukalas C, Mavroidi B, Paravatou-Petsotas M, Kalogeropoulos N, Xanthopoulos S, et al. (2020) A Proof-of-Concept Study on the Therapeutic Potential of Au Nanoparticles Radiolabeled with the Alpha-Emitter Actinium-225. *Pharmaceutics*, **12**(2): 188.
  27. Muslimov AR, Antuganov DO, Tarakanchikova YV, Zhukov MV, Nadporojkii MA, Zyuzin MV, Timin AS (2021) Calcium Carbonate Core-Shell Particles for Incorporation of (<sup>225</sup>Ac and Their Application in Local alpha-Radionuclide Therapy. *ACS Appl Mater Interfaces*, **13**(22): 25599-25610.